SUPPLEMENTARY INFORMATION

SUPPLEMENTARY METHODS

Crystallography

We initially attempted to solve the structure of IgFLNa19-21 using a KHgI derivative crystal that grew in space group P4(1)22. Datasets were collected in three different wavelengths (representative numbers for data quality are given in Table S1) and the multiple wavelength anomalous dispersion (MAD) method was used to locate two Hg atoms in the asymmetric unit of the crystal by using the programs SHELXD and SHELXE (Schneider and Sheldrick, 2002). The electron density map calculated based on the phases derived from the heavy atom position could be used to build two partial domains and an extra β strand connected to one of the domains, but the connections between these structures could not be unambiguously built.

In addition to the Hg derivative, several other approaches were also attempted including Se-Met labeled protein or KBr soaking to use Br ions bound to the protein for further phasing. The crystals diffracted typically to about 3.0 Å resolution, were non-isomorphic with each other, and belonged to either P4(1)22 or C222(1) space groups. Finally the best dataset of KBr soaked crystals could be used to 2.5 Å resolution in space group C222(1) and this could be solved by molecular replacement as described in the methods section of the manuscript. The structure was solved and refined with the CCP4 program package (Potterton *et al*, 2003). Solvent atoms were added to the model using the program ARP/wARP (Perrakis *et al*, 1999). Four dioxane molecules and one glycerol were included in the model.

To guard against model bias the molecular replacement solution was subjected to simulated annealing using the program CNS (Brunger *et al*, 1998). Furthermore, Arp/Warp (Perrakis *et al*, 1999) was used to build a dummy atom model based on the molecular replacement model phases and to automatically build part of the amino-acid sequence. Neither of these approaches revealed any large errors in the molecular replacement solution. Thus, the electron density map derived from the molecular replacement solutions was taken as a starting point for building the missing side chains in domain 19 and 21, domain 20 and connections between the three domains. In the final refinement the individual domains were defined as TLS groups so that the first strand of IgFLNa20 was included in the same group with the IgFLNa21 of the same chains. Thus, 6 TLS groups were used. Tight non-crystallographic symmetry (NCS) restrains were used in the final refinement between IgFLNa21+first stand of IgFLNA20 in chains A and B and between IgFLNa19 of chains A and B. The deposited pdb file contains the TLS tensor values for each of the TLS groups and residual isotropic B-factors for each atom. The total B-factor values shown in Figure 1B and in Table I were calculated with the program TLSANL (Howlin *et al*, 1993)

The Se-Met peak dataset (Table S1) was used for the validation of the partial model of IgFLNa20 so that an anomalous difference map was calculated using the phases derived from the final model. Similarly, anomalous difference map was calculated for the Br ions in the KBr-soaked crystal that was used for actual model building.

Molecular dynamics

For molecular dynamics simulation, the missing amino acid residues were added with Modeller8v2 (Sali and Blundell, 1993). The tleap module in antechamber (Wang *et al*, 2004; Wang *et al*, 2006) was used to produce: (i) the parm99 force field parameters for the protein, (ii) the solvation of system with 18 405 TIP3 waters extending 13 Å in all dimension around the solute, and (iii) the neutralization of system by adding 14 sodium ions.

Energy minimizations and MD simulations were performed using the NAMD (Phillips *et al*, 2005). First the system was equilibrated as follows. At first the energy minimization of the hydrogen atoms was performed by using the steepest descent algorithm (3000 steps). Followed by a similar minimization of all atoms with restrained C^{α}-atoms with a harmonic force of 5 $kcalmol^{-1}Å^{-2}$. Then a MD simulation was performed, first at constant volume (for 300 ps) and then at constant pressure (for a further 300 ps) for the whole system, with the C^{α}-atoms restrained as above. Finally, the whole system was equilibrated at constant pressure without any restrains for 450 ps. Finally a production simulation was performed for 10 ns. A constant pressure of 1 atm was maintained by using a Nosé-Hoover Langevin piston (Feller *et al*, 1995).

Time step of simulation was 2 fs, by using a multiple time stepping scheme (Schlick *et al*, 1999) where long-range electrostatic interactions were calculated only every third time step, while covalent and short-range interactions were computed every time step. A cutoff of 12 Å was used for van der Waals and short-range electrostatic interactions; a switching function was started at 10 Å for the van der Waals to ensure a smooth cutoff. The simulation was performed under periodic boundary conditions, with full-system, long-range electrostatics calculated by using the particle-mesh Ewald method. (Darden *et al*,

1993; Essmann *et al*, 1995; Sagui and Darden, 1999; Toukmaji *et al*, 2000). Bonds containing hydrogen atoms were constrained with the SHAKE algorithm. (Ryckaert *et al*, 1977). Trajectories obtained from the MD simulations were analyzed with ptraj6.5 (standalone version: www.chpc.utah.edu/~cheatham/software.html) and Bodil (Lehtonen *et al*, 2004) Figures were produced using Bodil (Lehtonen *et al.*, 2004).

SUPPLEMENTARY FIGURES

Figure S1. Validation of the IgFLNa model. Anomalous difference electron density calculated from a Se-Met labeled crystal of IgFLNa19-21 (green mesh, visualized at 4 σ) superimposes with the two Met residues present in IgFLNa20. No anomalous density was observed for the third Met residue (Met-1 in IgFLNa19) which is the 1st residue of the model.

Fig.S1

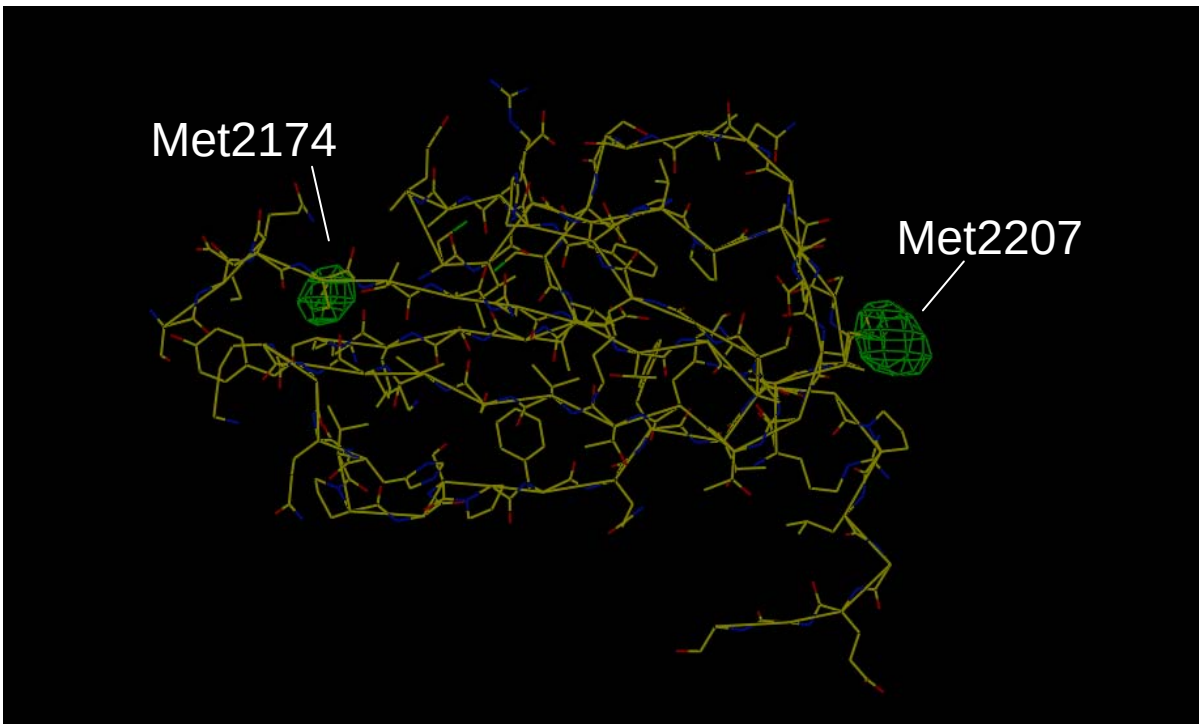

Figure S2. Molecular dynamics of IgFLNa19-21 reveals a rigid structure. **A.** The starting conformation of the IgFLNa19-21 (solid surface) is compared with a representative conformation at the end of simulation (transparent surface) so that IgFLNa21 (green) structures are superimposed. This comparison indicates that both IgFLNa20 (red) and IgFLNa19 (yellow) moved closer to IgFLNa21 during the simulation. This can be explained by stabilization of the domain-interactions. **B,C.** Details of the stabilization between IgFLNa20 and IgFLNa21 can be understood as a gap (indicated with an arrow in B) seen between IgFLN20 and IgFLN21 is closed during the MD simulation. **D,E.** Movement of IgFLNa20 (D) and IgFLNa19 (E) is also indicated as ribbon diagrams.

Fig.S2

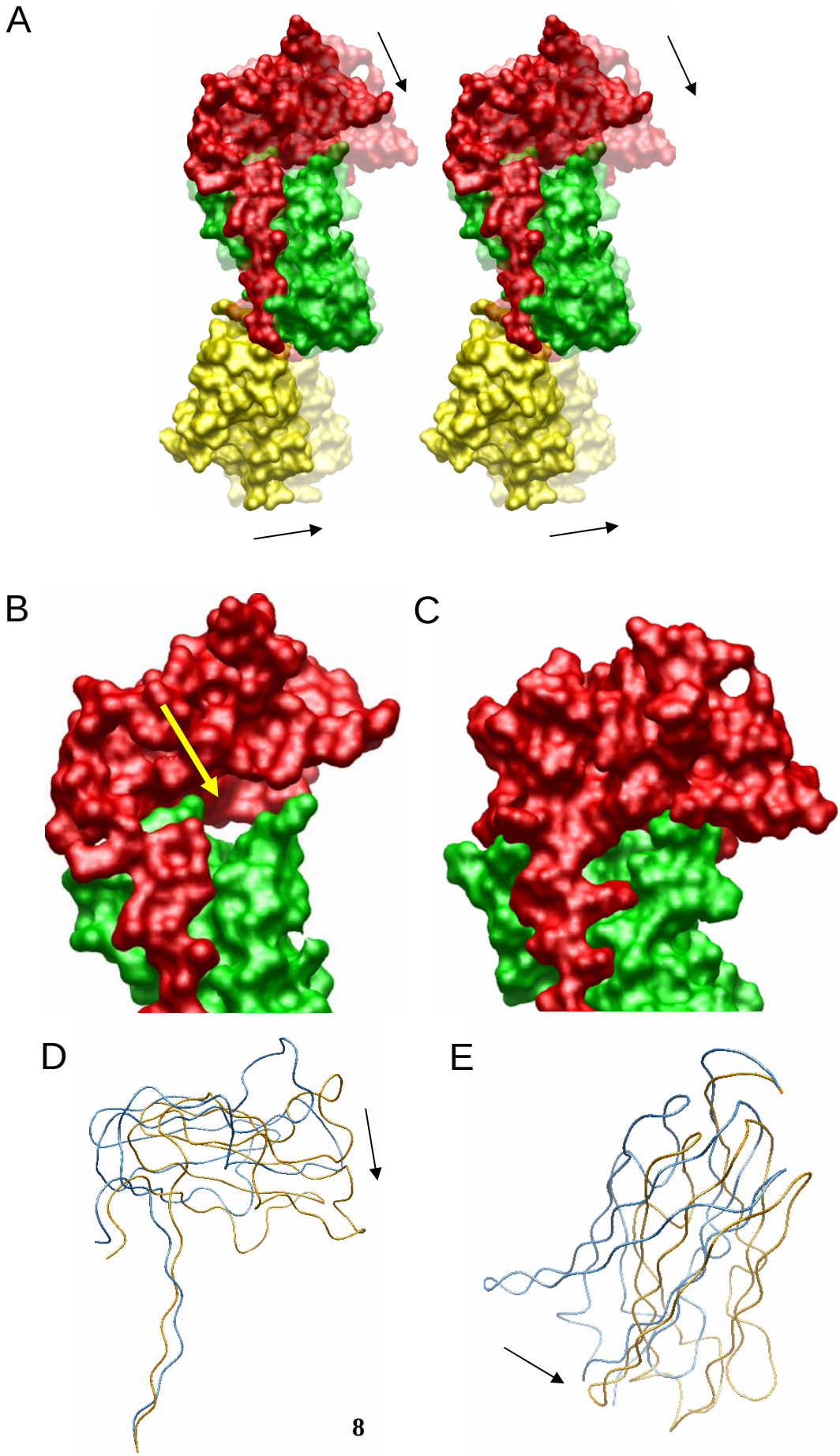

Figure S3. Competition between IgFLNa20 and integrin can be shown by NMR. Integrin β7 peptide can replace IgFLNa20 from an IgFLNa20-IgFLNa21 complex. A spectral superposition of IgFLNa21 (red), IgFLNa21+30×IgFLNa20 (gold), IgFLNa21+30×IgFLNa20+6×β7 (cyan), and IgFLNa21+6×β7 (purple) is shown. Initially, thirty-fold IgFLNa20 was added to IgFLNa21 alone. Next, six-fold β7 peptide was added to the same solution. As a reference, a six-fold β7 peptide was added to IgFLNa21 alone. The similarity of the triple component spectrum to that of the reference indicates that β7 is able to displace IgFLNa20 from the IgFLNa20-IgFLNa21 complex. IgFLNa21 has much stronger binding affinity for β7 than IgFLNa20, and integrin β7 can replace IgFLNa20 at a rather lower ratio; however the local concentration of IgFLNa20 and IgFLNa21 is very high when they are covalently attached.

The boxes show the isolated movement of peaks corresponding to two specific residues, which were chosen to exemplify the effects of ligand binding. S2279 is positioned on the loop between the C and D strands and E2301 on the loop between the E and F strands of IgFLNa21. The chemical environments of these two residues are seen to be significantly altered by ligand binding.

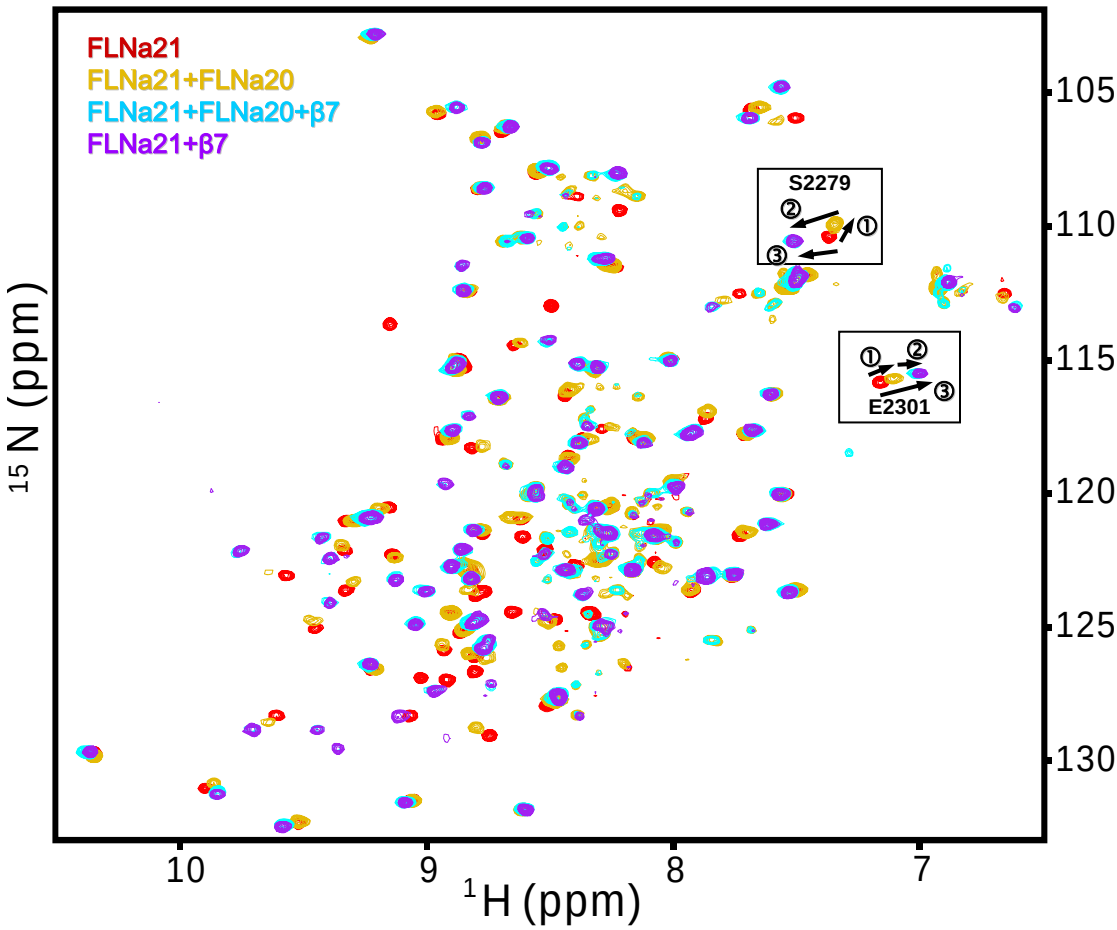
FLNa21
FLNa21+FLNa20
FLNa21+FLNa20+β7
FLNa21+β7
S2279
E2301
105
110
115
120
125
130
10
9
8
7
15 N (ppm)
1 H (ppm)

Figure S4.

Structure based sequence alignment of IgFLNa16-24 reveals sequence differences in the first strand and notably even-numbered domains 16, 18, 20 and 22 are most different. The residues that are identical in more than 50 % of sequences are boxed.

Fig.S4


16 APERPLVGVNGLDVTSLR
17 CGHVTAYGPGLTHGVVNK
18 GDDSMRMSHLKVGS
19 ASRVRVSGQGLHEGHTFE
20 KSITRRRRRAPSVANVGS
21 AHKVRAGGPGLERAEAGV
22 ARRLTVSSLQESGLKVNQ
23 PGLVSAYGAGLEGGVTGN
24 ASKVVAKGLGLSKAYVGQ

Table S1: Statistics of datasets collected[1]

	KHgI peak	SeMet Peak	KBr peak (used for final refinement)
Wavelength	1.0044 Å	0.97963	0.919750
Spacegroup	$P4_122$	$C222_1$	$C222_1$
Unit cell	53.14 Å, 53.14 Å, 231.19 Å 90^o 90^o 90^o	74.5 Å 74.8 Å 230.2 Å 90^o 90^o 90^o	72.3 Å 78.4 Å 229. Å 90^o 90^o 90^o
Resolution range	39.3-3.2 Å (3.3-3.2 Å)[2]	40-3.1 Å (3.2-3.1 Å)	43.3-2.5 Å (2.56-2.50 Å)
Rmerge	0.080 (0.301)	0.080 (0.297)	0.073 (0.267)
I/Sigma I	15.1 (5.45)	17.9 (6.54)	17.3 (3.95)
Number of reflection	10448	12079	20422
Completeness	100%	99.9%	98.7% (89.9%)
N:o of heavy atoms (found)	2[2][3]	6[0]	2[0]

[1]Only the KBr dataset was used for structure solution, SeMet dataset was used for validation (Figure S1).
[2]Values in parentheses correspond to the highest resolution shell
[3]Values in brackets indicate the number of heavy atoms found by the SHELXD program

SUPPLEMENTARY REFERENCES

Brunger,A.T., Adams,P.D., Clore,G.M., DeLano,W.L., Gros,P., Grosse-Kunstleve,R.W., Jiang,J.S., Kuszewski,J., Nilges,M., Pannu,N.S., Read,R.J., Rice,L.M., Simonson,T., and Warren,G.L. (1998). Crystallography & NMR system: A new software suite for macromolecular structure determination. *Acta Crystallogr. D. Biol. Crystallogr.,* **54:** 905-921.

Darden,T., York,D., and Pedersen,L. (1993). Particle mesh Ewald: An N [center-dot] log(N) method for Ewald sums in large systems. *The Journal of Chemical Physics,* **98:** 10089.

Essmann,U., Perera,L., Berkowitz,M.L., Darden,T., Lee,H., and Pedersen,L.G. (1995). A smooth particle mesh Ewald method. *The Journal of Chemical Physics,* **103:** 8577.

Feller,S.E., Zhang,Y., Pastor,R.W., and Brooks,B.R. (1995). Constant pressure molecular dynamics simulation: The Langevin piston method. *The Journal of Chemical Physics,* **103:** 4613.

Howlin,B., Butler,S.A., Moss,D.S., Harris,G.W., and Driessen,H.P.C. (1993). Tlsanl - Tls Parameter-Analysis Program for Segmented Anisotropic Refinement of Macromolecular Structures. *Journal of Applied Crystallography,* **26:** 622-624.

Lehtonen,J.V., Still,D., Rantanen,V., Ekholm,J., Björklund,D., Iftikhar,Z., Huhtala,M., Repo,S., Jussila,A., Jaakkola,J., Pentikäinen,O.T., Nyrönen,T., Salminen,T., Gyllenberg,M., and Johnson,M.S. (2004). BODIL: a molecular modeling environment for structure-function analysis and drug design. *Journal of Computer-Aided Molecular Design,* **V18:** 401.

Perrakis,A., Morris,R., and Lamzin,V.S. (1999). Automated protein model building combined with iterative structure refinement. *Nat Struct Biol,* **6:** 458-463.

Phillips,J.C., Braun,R., Wang,W., Gumbart,J., Tajkhorshid,E., Villa,E., Chipot,C., Skeel,R.D., Kale,L., and Schulten,K. (2005). Scalable molecular dynamics with NAMD. *J Comput Chem,* **26:** 1781-1802.

Potterton,E., Briggs,P., Turkenburg,M., and Dodson,E. (2003). A graphical user interface to the CCP4 program suite. *Acta Crystallogr D Biol Crystallogr,* **59:** 1131-1137.

Ryckaert,J.P., Ciccotti,G., and Berendsen,H.J.C. (1977). Numerical integration of the cartesian equations of motion of a system with constraints: molecular dynamics of n-alkanes. *Journal of Computational Physics,* **23:** 327.

Sagui,C. and Darden,T.A. (1999). Simulation and Theory of Electrostatic Interactions in Solution. In Pratt,L.R. and Hummer,G. (Eds.), *Simulation and Theory of Electrostatic Interactions in Solution: Computational Chemistry, Biophysics and Aqueous Solutions*, . American Institute of Physics, New York, pp. 104-113.

Sali,A. and Blundell,T.L. (1993). Comparative protein modelling by satisfaction of spatial restraints. *J Mol Biol,* **234:** 779-815.

Schlick,T., Skeel,R.D., Brunger,A.T., Kale,L.V., Board,J.A., Hermans,J., and Schulten,K. (1999). Algorithmic Challenges in Computational Molecular Biophysics. *Journal of Computational Physics,* **151:** 9.

Schneider,T.R. and Sheldrick,G.M. (2002). Substructure solution with SHELXD. *Acta Crystallogr. D. Biol. Crystallogr.,* **58:** 1772-1779.

Toukmaji,A., Sagui,C., Board,J., and Darden,T. (2000). Efficient particle-mesh Ewald based approach to fixed and induced dipolar interactions. *The Journal of Chemical Physics,* **113:** 10913.

Wang,J., Wang,W., Kollman,P.A., and Case,D.A. (2006). Automatic atom type and bond type perception in molecular mechanical calculations. *Journal of Molecular Graphics and Modelling,* **25:** 247.

Wang,J., Wolf,R.M., Caldwell,J.W., Kollman,P.A., and Case,D.A. (2004). Development and testing of a general amber force field. *J Comput Chem,* **25:** 1157-1174.